Shared-mode assisted resonant energy transfer in the weak coupling regime

E. Hennebicq,[1,2] D. Beljonne,[2] C. Curutchet,[3] G. D. Scholes,[3] and R. J. Silbey[1,a)]
[1]*Department of Chemistry, Massachusetts Institute of Technology, Cambridge, Massachusetts 02139, USA*
[2]*Chemistry of Novel Materials, University of Mons-Hainaut, Place du Parc 20, B-7000 Mons, Belgium*
[3]*Lash-Miller Chemical Laboratories, Institute for Optical Sciences and Centre for Quantum Information and Quantum Control, University of Toronto, 80 St. George Street, Toronto, Ontario M5S 3H6, Canada*

(Received 21 February 2009; accepted 1 May 2009; published online 2 June 2009)

Recent work has suggested that correlations in the environments of chromophores can lead to a change in the dynamics of excitation transfer in both the coherent and incoherent limits. An example of this effect that is relevant to many single molecule experiments occurs in the standard Förster model for resonant energy transfer (RET). The standard formula for the FRET rate breaks down when the electronic excitations on weakly interacting donor and acceptor couple to the same vibrational modes. The transfer rate can then no longer be factored into donor emission and acceptor absorption lineshapes, but must be recast in terms of a renormalized phonon reorganization energy accounting for the magnitude and sign of the excitation-vibration couplings. In this paper, we derive theoretically how the FRET rate depends on the shared mode structure and coupling, examine the simplified case of Gaussian lineshapes and then provide a quantitative calculation for a system of current interest. © *2009 American Institute of Physics*. [DOI: 10.1063/1.3140273]

I. INTRODUCTION

Resonant energy transfer (RET) is a nonradiative process involving the virtual exchange of a photon between an electronically excited chromophore [donor (D)] and another chromophore in its electronic ground state [acceptor (A)].[1] The dynamics along the intra- and intermolecular vibrational modes modulates the D-A electronic gap and RET proceeds when the vibrationally dressed D and A states are in resonance. In pioneering work, Förster connected the D emission and A absorption lineshape functions to the energy release by D deactivation and the simultaneously taking up of this excess energy by the A.[2,3] The [Förster (F)]RET transfer rate then scales linearly with the spectral overlap between the stationary D emission and A absorption spectra.[3]

Since the first application of Förster theory to weakly interacting chromophores,[4] the model has been successfully applied as an effective spectroscopic ruler in the 20–80 Å range to assess conformational equilibrium distributions from ensemble[5] and single molecule[6,7] FRET experiments. The Förster model is based on large D-A separations and weak electronic coupling in comparison to exciton-phonon interactions; however, many recent single molecule experiments have utilized systems with small D-A separations or even D-A dyads that are connected by a short bridge, necessitating a reexamination of the existing theory. In addition to the limitations inherent to the weak coupling approximation, deviations of the standard Förster model include the breakdown of the point dipole approximation for closely spaced chromophores or weakly allowed optical transitions,[8] distance-dependent dielectric screening of the electronic couplings by the environment,[9] the need to disentangle homogeneous (dynamic) and inhomogeneous (static) contributions to the lineshapes in the calculation of the spectral overlaps as well as the effect of multichromophoric arrays.[10]

In this paper, we examine a rather unexplored restriction of the Förster model that concerns the coupling of the vibrational modes in the calculation of the energy-conserving factor of the rate. The factorization of the spectral overlap into D and A spectral lines is based on the assumption of independent vibrational and phonon modes for D and A, which results from weak coupling and large separations. When the D and A have a common mode, the factorization fails, and the result for this mode resembles that of the Marcus model for electron transfer, which is derived on the basis of a *shared* vibrational mode. The aim of this paper is to derive theoretically how the FRET rate depends on the shared mode structure and coupling, and to provide a quantitative calculation for a system of current interest.

Recent papers have suggested that correlations in the environments of chromophores can lead to a change in the dynamics of excitation transfer in both the coherent and incoherent limits. Recent two-color photon-echo experiments on the bacterial reaction center (RC) system have revealed long-lasting (over ~500 fs) coherences between electronic states that result from a shared environment (rather than strong electronic coupling), so that the nearby chromophores vibrate in concert (thereby preserving the coherence).[11] The authors speculated that such long-lived electronic coherences may be responsible for the efficient excitation motion in the RC. The issue, however, of how the environmental correlations (e.g., vibrational mode correlations) depend on mode

a)Electronic mail: silbey@mit.edu.

structure and energy, and coupling to the excitations has not been studied quantitatively. A recent theoretical study[11] suggests that environmental correlations can have an effect on excitation dynamics, and concludes that a thorough discussion of the details is needed. In this paper, we quantitatively examine the dynamics of FRET for shared environments and show that the sharing (correlation) of environmental modes can lead to an increase or decrease in energy transfer rate, depending on the various parameters governing the excitation-vibration coupling.

We show that, in the incoherent limit, the existence of vibrational modes that are coupled simultaneously to D and A has a strong impact on the RET dynamics and lead to (i) a renormalization of the reorganization energy associated to the energy transfer process and (ii) the breakdown of the Förster relation between the energy transfer rate and the spectral overlap based on the lineshapes of the individual molecules. In order to indicate the effect in the starkest manner, consider the case in which the D and A excitations have *identical* vibrational modes and *identical* excitation-vibration coupling. Then during energy transfer, there can be *no* change in the vibrational state of the combined system, due to the orthogonality of the vibrational wave function. Hence there can be no energy conserving allowed transitions during energy transfer, and the rate is exactly zero. Of course, this situation is never the case in reality, but in many recent FRET experiments, the D and A can couple to the same vibrational modes due to the structure of the D-A dyad.

The paper is laid out as follows: in Sec. II, we present the theoretical model of excitation transfer when the D and A electronic excitations are coupled to a general set of vibrational modes. In Sec. III, we derive an analytic expression for the rate in the case of Gaussian lineshapes and compare this with the exact results for a specific mode. In Sec. IV, we apply the model to the calculation of FRET for phycocyanin chromophores that are covalently coupled to a protein scaffold. Finally, in Sec. V we conclude the discussion.

II. THEORETICAL ANALYSIS

The Förster derivation in the simple case of RET from a single D to a single A starts with the total Hamiltonian for the system: $H=H_D^e+H_A^e+H_b+H_D^{eb}+H_A^{eb}+V_{DA}a_D^\dagger a_A+V_{AD}a_A^\dagger a_D$, where H_D^e and H_A^e represent the electronic Hamiltonians for the D and the A, respectively; $a_D^\dagger(a_A^\dagger)$ and $a_D(a_A)$ are creation and annihilation operators for the vertical (bare) electronic excitation on the D (A) site; V_{DA} is the electronic coupling; H_b is the (harmonic) bath vibrational Hamiltonian; H_D^{eb} and H_A^{eb} account for linear excitation-phonon coupling for D and A. Treating V_{DA} to second order in perturbation and under the usual Förster assumptions (including the hypothesis that coherence is unimportant), the rate for energy transfer from D to A becomes[12]

$$k_{DA}=\frac{|V_{DA}|^2}{\hbar^2}\mathrm{Re}\int_{-\infty}^{+\infty}dt\left\{\begin{array}{c}\exp(i(\omega_{DA}^{0-0})t)^*\exp\left[-\sum_\lambda(g_\lambda^D-g_\lambda^A)^2(2\bar{n}(\omega_\lambda)+1)\right]\\ \exp\left[\sum_\lambda(g_\lambda^D-g_\lambda^A)^2[\bar{n}(\omega_\lambda)(\exp(i\omega_\lambda t))+(\bar{n}(\omega_\lambda)+1)\exp(-i\omega_\lambda t)]\right]\end{array}\right\},\tag{1}$$

where the dimensionless $g_\lambda^D(g_\lambda^A)$ exciton-phonon coupling factor is proportional to the displacement along vibrational mode λ of the D (A) excited state with respect to the ground-state geometry and $(g_\lambda^D)^2\hbar\omega_\lambda$ $((g_\lambda^A)^2\hbar\omega_\lambda)$ the corresponding reorganization energy; ω_{DA}^{0-0} denotes the energy gap between the D and A adiabatic transitions; $\bar{n}$ is the occupation number of the vibrational states. By making the assumption of independent modes (i.e., for each λ, either g^D or g^A is zero), Eq. (1) factors into a product of D $(\tilde{F}_D)$ and A $(\tilde{F}_A)$ lineshapes

$$\begin{aligned}k_{DA}&=\frac{1}{\hbar^2}|V_{DA}|^2\,\mathrm{Re}\int_{-\infty}^{+\infty}d\omega_1\tilde{F}_A(\omega_{DA}^{0-0}-\omega_1)\tilde{F}_D(\omega_1)\\&=\frac{1}{\hbar^2}|V_{DA}|^2\tilde{F}_{\mathrm{ov}}^F(\omega_{DA}^{0-0}),\end{aligned}\tag{2}$$

with $\tilde{F}_{\mathrm{ov}}^F(\omega_{DA}^{0-0})=\mathrm{Re}\int_{-\infty}^{+\infty}dt\,\exp(i(\omega_{DA}^{0-0})t)f_A(t)f_D(t)$ the Förster overlap factor obtained.

In the general case for which both local and shared modes are coupled to the electronic excitations, it is clear that k_{DA} will not factor into separate functions for A and D. In this case, the convolution theorem leads to a double convolution product expression for the overlap function:

$$\begin{aligned}\bar{F}_{\mathrm{ov}}^{\mathrm{NF}}(\omega_{DA}^{0-0})&=\mathrm{Re}\int_{-\infty}^{+\infty}dt\,\exp(i\omega_{DA}^{0-0}t)f_A(t)f_D(t)f_{DA}(t)\\&=\frac{1}{\sqrt{2\pi}}\mathrm{Re}\int_{-\infty}^{+\infty}d\omega_1\int_{-\infty}^{+\infty}d\omega_2\bar{F}_A(\omega_{DA}^{0-0}-\omega_1)\\&\quad\times\bar{F}_D(\omega_1-\omega_2)\bar{F}_{DA}(\omega_2),\end{aligned}\tag{3}$$

where the function $\tilde{F}_{DA}(\omega)$ involves those modes that are simultaneously coupled to D and A. Numerical simulations can either be done by expanding Eq. (1) into mode specific terms, or instead by considering the linear displaced Brownian harmonic oscillator model[13] in which the modes are partitioned into a set of primary modes linearly coupled to the electronic transitions; this set of primary modes then couple

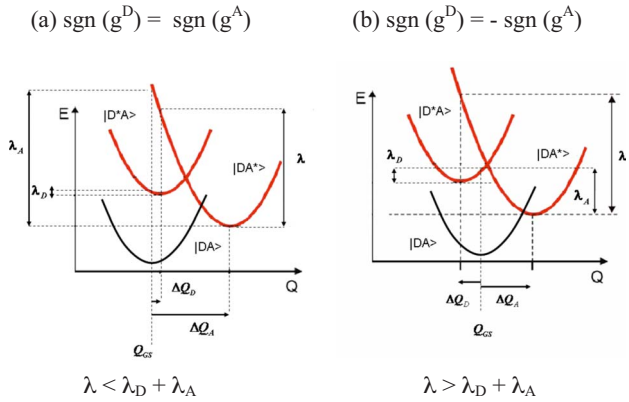

FIG. 1. (Color online) Schematic representation of the potential energy surfaces for ground state ($|DA\rangle$) and local excited states ($|D^*A\rangle$ and $|DA^*\rangle$) in the Gaussian approximation with same (a) and opposite (b) sign displacements.

to a set of harmonic oscillators characterized by their spectral densities. Damping of the primary modes due to the latter coupling then leads to convolution of their primary lineshapes [Eq. (3)] with Gaussian or Lorentzian profiles.

III. THE CASE OF GAUSSIAN LINESHAPES

In order to illustrate the effect simply, we derive an analytical expression for the RET rate in the case where a continuous distribution of low-frequency vibrational modes over the D and A leads to Gaussian lineshapes, before proceeding to exact numerical simulations. For independent Gaussian baths, the Förster overlap then becomes

$$\tilde{F}_{\mathrm{ov}}(\omega_{DA}^{0-0}) = \sqrt{\frac{2\pi}{\Sigma_\lambda((g_\lambda^D)^2+(g_\lambda^A)^2)\omega_\lambda[(2\bar{n}(\omega_\lambda)+1)\omega_\lambda]}} \times \exp\left(\frac{-\left((\omega_{DA}^{0-0})-\Sigma_\lambda((g_\lambda^D)^2+(g_\lambda^A)^2)\omega_\lambda\right)^2}{2\Sigma_\lambda((g_\lambda^D)^2+(g_\lambda^A)^2)\omega_\lambda[(2\bar{n}(\omega_\lambda)+1)\omega_\lambda]}\right). \quad (4)$$

This expression is similar to the Marcus charge transfer rate expression in the semiclassical limit.[14] The spectral overlap (and transfer rate) is maximized when the adiabatic D-A electronic gap is exactly compensated by the reorganization energy associated with the energy transfer process, which is simply the sum of the D and A relaxation energies: $\lambda_{\mathrm{ET}}=\Sigma_\lambda((g_\lambda^D)^2+(g_\lambda^A)^2)\omega_\lambda$. In the general case, the A lineshape must be convoluted with the effective D emission lineshape that itself results from the convolution between $\tilde{F}_D(\omega-\omega_1)$ and $\tilde{F}_{DA}(\omega_1)$. Applying the Gaussian approximation to Eq. (3) leads to an effective D emission lineshape that is shifted to larger (smaller) D-A transition energies for negative (positive) value of the cross terms $-2g_\lambda^D g_\lambda^A\omega_\lambda$. The spectral overlap takes the form of Eq. (4) where $((g_\lambda^D)^2+(g_\lambda^A)^2)\omega_\lambda$ is replaced with $((g_\lambda^D)^2+(g_\lambda^A)^2-2g_\lambda^D g_\lambda^A)\omega_\lambda$, i.e., after renormalization of the reorganization energy by the cross product. In the Gaussian model, the D and A potential energy surfaces (PES) are represented by the usual parabolas shown on Fig. 1 for a single discrete vibrational mode λ in the

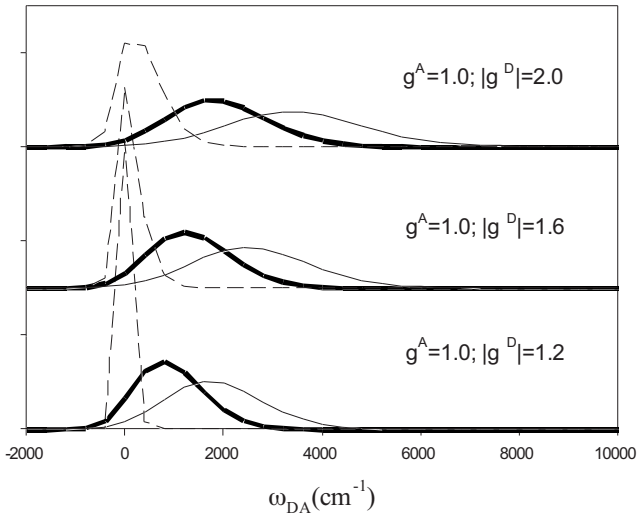

FIG. 2. Envelope of the effective spectral overlap as a function of the D-A electronic gap ω_{DA}^{0-0} for different values and signs of the electron-phonon couplings g_λ^D and g_λ^A. The thick line is the Förster result. The thin and dashed lines correspond to displacements with opposite and same signs, respectively. $T=300$ K and $\omega_\lambda=400$ cm^{-1}.

cases: $\mathrm{sgn}(g_\lambda^D)=\mathrm{sgn}(g_\lambda^A)$ and $\mathrm{sgn}(g_\lambda^D)=-\mathrm{sgn}(g_\lambda^A)$. It is readily seen from Fig. 1 that, in comparison to the Förster limit, the reorganization energy for RET is reduced in the former case (same sign displacements) and increased in the latter (opposite sign displacements).

To quantify these effects, we have computed the room temperature functions for $\tilde{F}_{\mathrm{ov}}^F(\omega_{DA}^{0-0})$ and $\tilde{F}_{\mathrm{ov}}^{\mathrm{NF}}(\omega_{DA}^{0-0})$ using the exact Eq. (3) for a single discrete mode with $\omega_\lambda=400$ cm^{-1} (chosen for illustrative purposes only) and different values for g_λ^D and g_λ^A. As expected from the Gaussian approximation, the overlap function is shifted to larger (smaller) D-A transition energies when g_λ^D and g_λ^A have opposite (same) signs (Fig. 2). In addition, as the total reorganization energy is larger (smaller) in the case of opposite (same) sign displacements, the effective overlap function extends over a broader (narrower) range of ω_{DA}^{0-0} values compared to the Förster overlap. Figure 3 portrays the value of

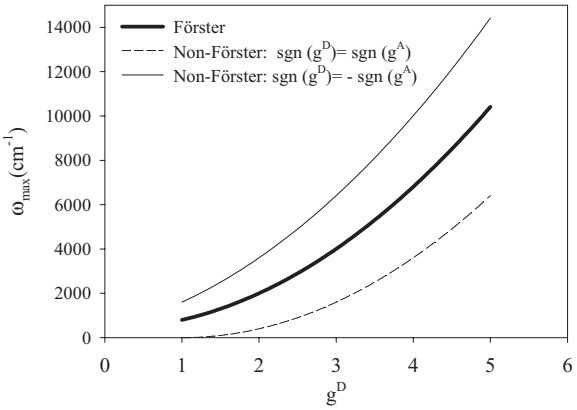

FIG. 3. Value of the D-A electronic gap ω_{DA}^{0-0} that maximizes the spectral overlap factor as a function of the excitation-phonon coupling g_λ^D on the D in the case of: (i) independent modes (Förster case, thick line); (ii) one single nonlocal vibrational mode (non-Förster case, with $g_\lambda^A=1$ and opposite sign displacements, thin line); (iii) same as (ii) for same sign displacements (dashed line). $\omega_\lambda=400$ cm^{-1} and $T=300$ K.

ω_{DA}^{0-0} that maximizes the renormalized overlap for the different cases. It is seen that for given values of g_λ^D and g_λ^A, which completely determine the D emission and A lineshapes, the peak in spectral overlap, and hence energy transfer rate is achieved for a larger (smaller) energy mismatch between D and A adiabatic excitation energies when the minima in the excited D and A PES are displaced in opposite (same) directions with respect to the ground state. g_λ^D and g_λ^A have opposite signs, a significant effective overlap could thus result from coupling of the electronic excitation to such nonlocal modes despite a large D-A electronic gap, while this would be precluded at the Förster level. Note, that a shared vibrational mode with $g_\lambda^D = g_\lambda^A$ would not be coupled at all to the energy transfer process although it would contribute to the spectral lineshapes of the individual D and A spectra; thus, once again the simple Förster model would be in error.

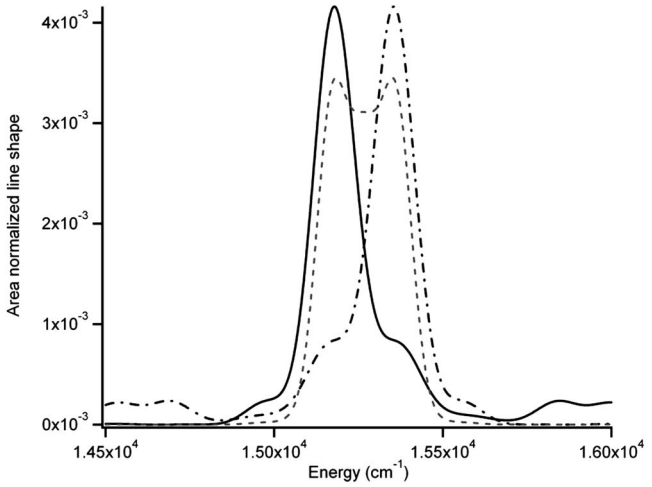

FIG. 4. Spectral overlap (dashed line) of the area-normalized D emission lineshape (dash-dotted line) and area-normalized A absorption lineshape (solid line) for the two low energy bilins of phycocyanin 645 (PC645) from cryptophyte algae Chroomonas CCMP270. Lineshapes correspond to D and A transition energies of 1.94 and 1.92 eV, respectively (see text for details).

IV. APPLICATION TO A MODEL D-A DYAD: BILIN CHROMOPHORES

Photosynthetic proteins have proven to be excellent model systems for learning about the mechanism and dynamics of RET. In addition, recent experimental evidence suggests that protein modes shared among different chromophores of the bacterial RC play an active role in protecting electronic coherences between their electronic states.[11] In contrast to the RC, the chromophores in biliproteins are covalently bonded to the protein scaffold, so the role of protein shared modes could be even more significant in these systems. Therefore, we have next performed numerical simulations of the spectral overlap, including the possibility that a single mode is shared, on a model D-A system comprising the two lowest energy bilin chromophores of phycocyanin 645 (PC645) from the cryptophyte algae *Chroomonas CCMP270*. The D and A lineshapes are taken to be a sum of two overdamped Brownian oscillators (BOs), representing the homogeneous line broadening due to the low frequency environmental modes, and a sum of discrete oscillators (DOs), describing intramolecular vibrations. We use transition energies of 1.94 and 1.93 eV for D and A, respectively, corresponding to the values estimated from Ref. 15 (DO and BO line functions are calculated at 298 K according to Eqs. 8.39 and 8.49 of Ref. 13). In addition, we consider spectral overlaps for model cases where the transition energy of the A is shifted to 1.92 and 1.91 eV.

Figure 4 shows the standard spectral overlap obtained from the D and A lineshapes, assuming no shared modes. In Tables I and II we report spectral overlap factors calculated for various cases where we consider none or one single BO or DO mode to be shared between D and A. In particular, in the results of Table I (II) we assume opposite (same) sign displacements for the shared mode. We are aware that intramolecular vibrations should be localized on single chromophores, whereas a low frequency environmental mode has more chances to be shared in the PC645 system. However, we also explore the possibility of common DO modes because this may occur in some situations, for instance, due to coupling to the intermolecular vibrations via the protein backbone.

Interestingly, the results in Table I show that the presence of a shared mode with *opposite* sign displacements leads to significant *decreases* in the effective overlap. In particular, variations as large as -40% are predicted for the case of common DO modes, while environmental modes lead to smaller (-10%) variations that progressively disappear when the main peaks of the chromophores overlap poorly ($\omega_A = 1.91$ eV). In contrast, the presence of a shared mode with the *same* sign displacements leads in most cases to net *increases* in the effective overlap, as shown in Table II. Again, DO modes induce variations that can be significant ($\sim 70\%$) while BO modes are expected to cause smaller changes ($<20\%$). It is also interesting to analyze the impact of high and low frequency shared modes as the position of the main peaks in the chromophores is shifted. When ω_A is 1.93 eV, the two peaks overlap very well, and increases of $\sim 10\%-40\%$ are predicted for the overlap factor when a BO or a low frequency DO mode is shared. However, when ω_A is redshifted to 1.92 or 1.91 eV, this effect progressively becomes negligible. On the contrary, the impact of sharing high frequency vibrations progressively increases as the overlap between the main peaks worsens, especially in the case of same sign displacements. This behavior can be explained due to the more important role of the vibrational side peaks in these latter spectral overlaps, compared to the previous one, where the main peaks overlap very well. Thus, the absence/presence of shared modes in the FRET expression can increase/decrease the effective overlap and the energy transfer rate because of the shared environment. These simulations indicate that the presence of nonlocal vibrational modes should result in the scattering of the transfer rates as a function of Förster overlaps owing to the fluctuations in the "effective" spectral overlaps across the inhomogenous ensemble.

TABLE I. Spectral overlap factors between the two low energy bilins of PC645 obtained by assuming independent nuclear modes or the possibility that one mode is shared between donor and acceptor assuming *opposite* sign displacements. Donor transition energy is 1.94 eV, while acceptor one is taken to be 1.93, 1.92, and 1.91 eV. The column labeled "% change" gives the percentage change from value of F with no shared mode and the value of F in that row.

	$\omega_A=1.93$ eV		$\omega_A=1.92$ eV		$\omega_A=1.91$ eV	
Shared mode[a]	$\tilde{F}_{ov}$ (10^{-3} cm)	% change	$\tilde{F}_{ov}$ (10^{-3} cm)	% change	$\tilde{F}_{ov}$ (10^{-3} cm)	% change
None	2.01	···	1.50	···	1.01	···
BO 1	1.81	−10	1.38	−8	0.982	−3
BO 2	1.80	−10	1.50	0	1.04	3
DO 1	1.73	−14	1.49	−1	1.05	4
DO 2	1.41	−30	1.16	−22	1.02	1
DO 3	1.45	−28	0.965	−36	0.656	−35
DO 4	1.50	−26	0.993	−34	0.676	−33
DO 5	1.32	−34	0.900	−40	0.581	−42
DO 6	1.68	−17	1.11	−26	0.766	−24
DO 7	1.40	−30	0.944	−37	0.620	−39
DO 8	1.84	−9	1.23	−18	0.856	−15

[a]Donor and acceptor lineshape functions taken to be a sum of two overdamped Brownian oscillators (BOs), each with reorganization energy $\lambda=130$ cm^{-1} and modulation frequencies $\Lambda_1=20$ ps^{-1} and $\Lambda_2=0.67$ ps^{-1}; and a sum of discrete oscillators (DOs) with frequencies in cm^{-1} (exciton-phonon coupling factors): 10 (0.5), 200 (0.1), 665 (0.05), 818 (0.04), 1108 (0.04), 1270 (0.02), 1370 (0.03), and 1645 (0.01) (values estimated in Ref. 15). Discrete oscillators are numbered in order of increasing frequency.

V. CONCLUSIONS

To conclude, we have shown how the presence of common vibrational modes for the donor and acceptor predicts a renormalized reorganization energy for RET and the breakdown of the standard Förster model. In particular, the strict requirement of spectral overlap between the emission spectrum of a donor and the absorption spectrum of an acceptor, at the heart of Förster theory, is relaxed if modes couple simultaneously to the donor and acceptor electronic excitations with opposite sign displacements. We have extended the Förster model to account for these nonlocal vibrational modes and the model has been applied to quantify the resulting changes in overlap factors and energy transfer rates for phycocyanin chromophores. Note that the expression for the terms for shared modes resembles that found in the Marcus expression for electron transfer, since in the latter model the coordinates that affect the electron transfer rate are just those that are shared between the donor and acceptor electronic

TABLE II. Spectral overlap factors between the two low energy bilins of PC645 obtained by assuming independent nuclear modes or the possibility that one mode is shared between donor and acceptor assuming *same* sign displacements. Donor transition energy is 1.94 eV, while acceptor one is taken to be 1.93, 1.92, and 1.91 eV. The column labeled "% change" gives the percentage change from value of F with no shared mode and the value of F in that row.

	$\omega_A=1.93$ eV		$\omega_A=1.92$ eV		$\omega_A=1.91$ eV	
Shared mode[a]	$\tilde{F}_{ov}$ (10^{-3} cm)	% change	$\tilde{F}_{ov}$ (10^{-3} cm)	% change	$\tilde{F}_{ov}$ (10^{-3} cm)	% change
None	2.01	···	1.50	···	1.01	···
BO 1	2.20	9	1.73	15	1.00	−1
BO 2	2.38	18	1.39	−7	0.995	−1
DO 1	2.73	36	1.18	−22	1.05	4
DO 2	2.77	38	2.51	67	1.12	11
DO 3	1.86	−8	2.20	47	1.55	53
DO 4	1.83	−9	2.14	43	1.50	49
DO 5	1.53	−24	2.19	46	1.70	68
DO 6	1.90	−6	1.97	32	1.33	32
DO 7	1.58	−21	2.14	43	1.61	59
DO 8	1.99	−1	1.80	20	1.19	18

[a]Donor and acceptor lineshape functions taken to be a sum of two overdamped Brownian oscillators (BOs), each with reorganization energy $\lambda=130$ cm^{-1} and modulation frequencies $\Lambda_1=20$ ps^{-1} and $\Lambda_2=0.67$ ps^{-1}, and a sum of discrete oscillators (DOs) with frequencies in cm^{-1} (exciton-phonon coupling factors): 10 (0.5), 200 (0.1), 665 (0.05), 818 (0.04), 1108 (0.04), 1270 (0.02), 1370 (0.03), and 1645 (0.01) (values estimated in Ref. 15). Discrete oscillators are numbered in order of increasing frequency.

states. Thus the correct FRET expression for the case of shared modes has partial "Marcus" character and partial "Förster" character.

ACKNOWLEDGMENTS

The authors gratefully acknowledge the Belgian National Fund for Scientific Research (FNRS-FRFC) and the European STREP project MODECOM (Grant No. NMP-CT-2006-016434) for financial support. E.H. and D.B. are FNRS postdoctoral research fellow and research associate, respectively. R.J.S. acknowledges partial support from the NSF under Grant No. CHE0556268. The work in Toronto was supported by the Natural Sciences and Engineering Research Council of Canada. G.D.S. acknowledges the support of an E. W. R. Steacie Memorial Fellowship.

[1] Th. Förster, in *Modern Quantum Chemistry, Istanbul Lectures, Part III: Action of Light and Organic Crystals*, edited by O. Sinanoglu (Academic, New York, 1965), p. 93.
[2] Th. Förster, Discuss. Faraday Soc. **27**, 7 (1959); Naturwiss. **33**, 166 (1946).
[3] Th. Förster, Ann. Phys. **437**, 55 (1948).
[4] L. Stryer and R. P. Haugland, Proc. Natl. Acad. Sci. U.S.A. **58**, 719 (1967).
[5] P. R. Selvin, Nat. Struct. Biol. **7**, 730 (2000).
[6] W. E. Moerner and M. Orrit, Science **283**, 1670 (1999).
[7] S. Weiss, Science **283**, 1676 (1999).
[8] G. D. Scholes, Annu. Rev. Phys. Chem. **54**, 57 (2003).
[9] G. D. Scholes, C. Curutchet, B. Mennucci, R. Cammi, and J. Tomasi, J. Phys. Chem. B **111**, 6978 (2007).
[10] G. D. Scholes, X. J. Jordanides, and G. R. Fleming, J. Phys. Chem. B **105**, 1640 (2001); S. Jang, J. Chem. Phys. **127**, 174710 (2007); K. Mukai, A. Abe, and H. Sumi, J. Phys. Chem. B **103**, 252 (1999); **103**, 6096 (1999); S. Jang, M. D. Newton, and R. J. Silbey, Phys. Rev. Lett. **92**, 218301 (2004); C. Didraga, V. A. Malyshev, and J. Knoester, J. Phys. Chem. B **110**, 18818 (2006).
[11] H. Lee, Y.-C. Cheng, and G. R. Fleming, Science **316**, 1462 (2007); F. Caruso, A. W. Chin, A. Datta, S. F. Huelga, and M. B. Plenio, e-print arXiv:cond-mat/0901.4454v1.
[12] V. May and O. Kühn, *Charge and Energy Transfer in Molecular Systems* (Wiley-VCH, Berlin, 2000).
[13] S. Mukamel, *Principles of Nonlinear Optical Spectroscopy* (Oxford University Press, New York, 1995).
[14] B. Li, A. E. Johnson, S. Mukamel, and B. Myers, J. Am. Chem. Soc. **116**, 11039 (1994).
[15] T. Mirkovic, A. B. Doust, J. Kim, K. E. Wilk, C. Curutchet, B. Mennucci, R. Cammi, P. M. G. Curmi, and G. D. Scholes, Photochem. Photobiol. Sci. **6**, 964 (2007).